Directed flow in ultrarelativistic heavy-ion collisions

Piotr Bożek[1,2,*] and Iwona Wyskiel[1]
[1]*The H. Niewodniczański Institute of Nuclear Physics, PL-31-342 Kraków, Poland*
[2]*Institute of Physics, Rzeszów University, PL-35-959 Rzeszów, Poland*
(Received 26 February 2010; published 11 May 2010)

We study the generation of the directed flow in the hydrodynamic expansion of hot matter formed in ultrarelativistic heavy-ion collisions at $\sqrt{s} = 200$ GeV. The experimentally observed negative-directed flow in a wide range of central pseudorapidities is reproduced, assuming that the fireball is tilted away from the collision axis. The tilt of the source is consistent with a preferential emission in the forward-backward hemisphere from forward-backward participating nucleons. The model reproduces the experimentally observed scaling of the directed flow when going from Au-Au to Cu-Cu systems.

DOI: 10.1103/PhysRevC.81.054902 PACS number(s): 25.75.Ld, 24.10.Nz, 24.10.Pa

I. INTRODUCTION

The appearance of the transverse, azimuthally asymmetric flow is one of the key observations in the physics of relativistic heavy-ions [1]. It proves that a collectively expanding, strongly interacting medium is formed in the course of the reaction. A number of observables have been studied, both in experiments, and in model calculations, in order to unravel the properties of the dense hot matter created in the collisions. The production of particles with soft momenta can be interpreted as a thermal emission of particles from fluid elements moving with some collective velocity field [2]. Relativistic hydrodynamics describes quantitatively the development of the collective velocity from pressure gradients in the fireball [3–5].

For noncentral collisions, the interaction region is azimuthally asymmetric and, as a result of the collective expansion of matter, azimuthally asymmetric emission of particles takes place. The effect can be quantified in terms of Fourier coefficients in the expansion of the measured particle spectra

$$\frac{dN}{d^2p_\perp d\eta} = \frac{dN}{2\pi p_\perp dp_\perp d\eta}[1 + 2v_1\cos(\phi) + 2v_2\cos(2\phi) + \cdots]. \quad (1)$$

The elliptic flow coefficient v_2 is known to be a very sensitive probe of the pressure in the system at early stages [6].

Directed flow, quantified by the coefficient v_1, is also measured at energies available at the BNL Relativistic Heavy Ion Collider (RHIC). The coefficient v_1 of the directed flow is zero at zero rapidity for collisions of symmetric nuclei, but it increases when moving to forward or backward pseudorapidities η. Its size and sign has been the subject of many studies at lower energies, where it is dominated by nucleon flow [7]. At RHIC energies, the spectator nucleons have positive directed flow ($v_1 > 0$ for $\eta > 0$), resulting from the deflection of the spectators during the collision. On the other hand, matter in the fireball shows a significant negative (antiflow) component for pseudorapidities $-4 < \eta < 4$ and for centralities $c = 0\% - 80\%$, both for Cu-Cu and Au-Au collisions [8–10]. A striking characteristic of the measured directed flow is the large negative value of v_1 even at the highest energy $\sqrt{s} = 200$ GeV. Another important observation is the scaling of the measured directed flow with the size of the system. The coefficient v_1 is the same for both systems (Au-Au or Cu-Cu), for the same centrality. Whereas, a scaling of v_2 with the density of the fireball has been observed [11].

Transport models of nuclear reactions describe the directed flow at lower energies, but generally underpredict the amount of antiflow at RHIC energies at central rapidities [12]. On the other hand, these calculations predict a large negative flow at large rapidities. Some calculations [13] predict significant antiflow around central rapidities, larger than observed, but yield a positive flow for $|\eta| > 3$, unlike that observed in experiments. It has been noticed that the appearance of negative-directed flow around central rapidities could be an effect of the softening of the equation of state [14]. This effect is called the third flow component. Hydrodynamic calculations incorporating such effects yield a negative elliptic flow at central rapidities and a positive directed flow at larger pseudorapidities, unlike the experimental data. A hydrodynamic calculation with initial conditions from a microscopic model gives the correct sign, but a magnitude of the directed flow that is too small for central rapidities [15].

There are two effects leading to a negative-directed flow in the models. The first one is the shadowing of the fireball matter by the spectators, which can give a substantial negative v_1 for $|\eta| > 4$. The second one is the build up of the flow away from the collision axis due to a tilt of the source. The description of the magnitude of the directed flow at different centralities for central rapidities requires a tilt of the source of the right magnitude as a function of the impact parameter and a sufficient amount of collectivity to generate the flow. We consider two initial conditions for the hot source in the hydrodynamic evolution. The first one is the most commonly used initial conditions in $(3 + 1)$-dimensional $[(3 + 1)\text{D}]$ calculations incorporating a Bjorken flow in the longitudinal direction and a shift in space-time rapidity due to the local imbalance of the momentum [4]. The second one assumes that the initial density results from a superposition of the energy density radiated by the color sources in the target and the projectile. The preferred emission in the pseudorapidity

*Piotr.Bozek@ifj.edu.pl

 ©2010 The American Physical Society

hemisphere of the emitting charge results in a tilt of the source for noncentral collisions. We show that the second choice leads to a satisfactory description of the directed flow generated in heavy ion collisions at $\sqrt{s} = 200$ GeV for central rapidities.

II. INITIAL CONDITIONS AND EARLY FLOW

Hydrodynamic evolution in $(3 + 1)$D at RHIC energies is performed in the proper time $\tau = (t^2 - z^2)^{1/2}$. The densities are defined as functions of the transverse plane $(x$-$y)$ coordinates and the space-time rapidity $\eta_\parallel = \frac{1}{2}\log[(t + z)/(t - z)]$. The hydrodynamic model requires some initial density and initial flow profile to be chosen at the initial time τ_0. Although some guidance from microscopic models of elementary collisions is possible in the choice of the initial conditions, there is still a vast choice of initial energy density profiles that are used in the simulations. Also, most of the calculations assume a Bjorken initial flow in the longitudinal direction and no initial transverse flow:

$$u^\mu(\tau_0, x, y, \eta_\parallel) = (\cosh\eta_\parallel, 0, 0, \sinh\eta_\parallel). \tag{2}$$

In the hydrodynamic evolution, the generation of the left-right asymmetry of the flow in the two (forward-backward) halves of the reaction plane requires the presence of an asymmetry in the initial distributions. For noncentral collisions, the azimuthal asymmetry of the interaction region results in a nonzero initial eccentricity in the transverse plane that gives rise to the collective elliptic flow. For collisions of symmetric nuclei and neglecting the fluctuations, the odd components of the decomposition in Fourier coefficients vanish at space-time rapidity zero. At forward and backward rapidities, an imbalance between the contributions from the target and the projectile to the initial source can result in a left-right deformation of the source in the transverse plane or in an asymmetric initial flow that could generate collective directed flow.

The observation of nonzero directed flow implies that the symmetry in the reaction plane is indeed broken, either in the initial flow or in the initial density, or both. We tried to reproduce the observed directed flow assuming an asymmetric initial flow, different from the Bjorken one of Eq. (2), but without success. Therefore, in the following we assume a Bjorken initial flow and study the effect of asymmetric initial densities on the directed flow.

Starting with a factorized initial energy density in the transverse plane and in the space-time rapidity

$$\epsilon(\eta_\parallel, x, y) = \rho(x, y) f(\eta_\parallel), \tag{3}$$

the subsequent evolution remains symmetric with respect to the $\eta_\parallel$ axis in the reaction plane $(\eta_\parallel$-$x)$, with the consequence that the directed flow is exactly zero. Factorized initial conditions in the Glauber model imply that all the participant nucleons or binary collisions contribute in a similar way to the total density, with a longitudinal profile proportional to $f(\eta_\parallel)$.

Modifications of the symmetric distribution of Eq. (3) could happen during the formation of the initial thermalized state. Momentum imbalance between left- and right-going participants at a given point in the transverse plane results in a nonzero total momentum of the matter. The longitudinal distribution is shifted in space-time rapidity [4,16] by the value of the center of mass rapidity of the fluid:

$$\eta_{\rm sh} = \frac{1}{2}\log\left[\frac{N_+ + N_- + v_N(N_+ - N_-)}{N_+ + N_- - v_N(N_+ - N_-)}\right], \tag{4}$$

where N_+ and N_- are the densities of participants from the two nuclei and v_N is the velocity of the incident nuclei.

$$N_+(x, y) = T(x - b/2, y)\left\{1 - \exp\left[-\frac{\sigma T(x + b/2, y)}{A}\right]\right\}$$
$$N_-(x, y) = T(x + b/2, y)\left\{1 - \exp\left[-\frac{\sigma T(x - b/2, y)}{A}\right]\right\}, \tag{5}$$

where σ is the cross section,

$$T(x, y) = \int dz \rho(x, y, z) \tag{6}$$

is the thickness function calculated from the Woods-Saxon density of colliding nuclei

$$\rho(x, y, z) = \frac{\rho_0}{1 + \exp\left[(\sqrt{x^2 + y^2 + z^2} - R_A)/a\right]}. \tag{7}$$

We use the same parameters as in Ref. [5], where a satisfactory description of spectra and femtoscopy data for Au-Au collisions at $\sqrt{s} = 200$ GeV has been obtained. The initial energy density takes the form [4,16]

$$\epsilon(\tau_0) = \epsilon_0 f(\eta_\parallel - \eta_{\rm sh})\{[N_+(x, y) + N_-(x, y)](1 - \alpha) + 2\alpha N_{\rm bin}(x, y)\}/N_0\,. \tag{8}$$

The relative contribution from binary collisions is $\alpha = 0.145$, with $N_{\rm bin}(x, y) = \sigma T(x - b/2, y)T(x + b/2, y)$. In the following, we call these initial conditions shifted initial conditions (Fig. 1).

The form of the initial energy density profile $f(\eta_\parallel)$ is adjusted to reproduce the measured charged-particle distribution in pseudorapidity. The resulting width of the initial

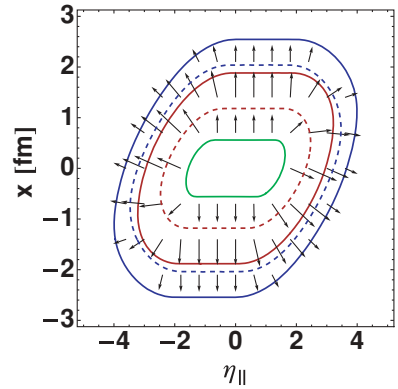

FIG. 1. (Color online) Contour plot of the initial pressure $p(\eta, x, y = 0)$ in the fireball for the shifted densities [Eq. (8)]. Solid lines correspond to the pressure of 9, 3, and 1 GeV/fm^3 for Au-Au collisions (impact parameter $b = 11$ fm) and dashed lines to the pressure of 3 and 1 GeV/fm^3 for Cu-Cu collisions ($b = 7.6$ fm). The arrows represent the gradient $(-\partial_\eta p/\tau_0, -\partial_x p)$ for Au-Au collisions in arbitrary units.

distribution depends on the chosen equation of state, initial time τ_0, and shear viscosity [5,17]. In the following we use ideal fluid hydrodynamics with $\tau_0 = 0.25$ fm/c and a realistic, hard equation of state [18], which requires

$$f(\eta_\parallel) = \exp\left[-\frac{(\eta_\parallel - \eta_0)^2}{2\sigma_\eta^2}\theta(|\eta_\parallel| - \eta_0)\right], \tag{9}$$

with a plateau of width $2\eta_0 = 2.0$ and $\sigma_\eta = 1.3$.

A different type of initial conditions studied in this work assumes a preferred emission from participating nucleons in the same hemisphere. Instead of a symmetric distribution of matter in space-time rapidity given by the function $f(\eta_\parallel)$ in Eq. (3), we assume that the deposited energy depends on the rapidity of the emitting participating nucleon. Such a distribution depending on the rapidity difference between the emitting charge and the emitted gluon is assumed in some phenomenological models [19]. However, there is no direct measurement of the contribution to soft-particle production from a single forward- or backward-moving charge. A phenomenological analysis is possible, by comparing multiplicity distributions in pseudorapidity for different asymmetric systems or by studying multiplicity correlations in different pseudorapidity intervals. These studies indicate that a preferred emission for rapidities close to the rapidity of the participating charge occurs [20–23]. In the wounded nucleon model of nuclear collisions, such correlations can be understood as due to a specific distribution of soft particles produced by each participant nucleon. Nucleons from the projectile [with positive rapidity $y_B = \ln(\sqrt{s}/m_N) > 0$] emit more particles in the forward ($\eta > 0$) than in the backward hemisphere. The form of the extracted charged particle distribution can be approximated by the function

$$f_F(\eta) = \frac{\eta + \eta_m}{2\eta_m} \tag{10}$$

in the interval $[-\eta_m, \eta_m]$, where $\eta_m = y_b - \eta_s$ defines the range of rapidity correlations; at $\sqrt{s} = 200$ GeV it is $\eta_m \sim y_b - 2 \simeq 3.36$. The origin of the shift in rapidity $\eta_s \simeq 2$ is not understood [20,21]. For practical purposes, we can treat it as a phenomenological parameter. Particle production in the remaining pseudorapidity intervals close to the fragmentation regions $[\eta_m, y_b]$ and $[-y_b, -\eta_m]$ cannot be reliably described in a hydrodynamic model anyway. Within the framework of relativistic hydrodynamics, we are interested in describing the main characteristics of the soft part of particle spectra in the central region $-3.5 < \eta < 3.5$ and, in particular, the directed flow. There is another reason why the phenomenological estimates of the emission of particles from participant nucleons [20,21] cannot be directly translated into the initial conditions for hydrodynamics that we are interested in. References [20,21] study particle distributions and correlations in the final state, whereas we know that, in realistic hydrodynamic simulations, the matter distribution in space-time rapidity evolves during the expansion of the fireball [5,17]; also statistical emission broadens the distribution in pseudorapidity. It means that the initial profile $f(\eta_\parallel)$ is significantly narrower than the final charged particle distribution $dN/d\eta$. The correlation functions in pseudorapidity [21] can be modified due to the longitudinal transport and the generation of

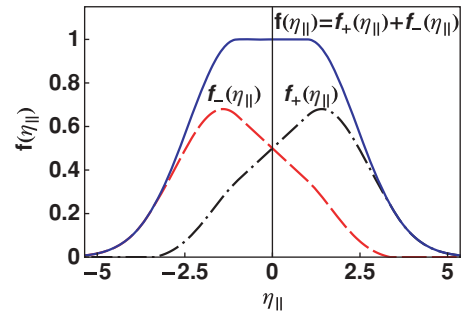

FIG. 2. (Color online) Initial profile in the longitudinal (space-time rapidity) direction. The symmetric function $f(\eta_\parallel)$ is composed of the two contributions f_+ and f_- representing the emission from forward- and backward-going participant nucleons.

transverse flow as well. We propose as a phenomenological ansatz (Fig. 2), inspired by the observations in Refs. [20–23], that the initial energy density of matter produced by a single participant nucleon of rapidity y_b is proportional to

$$f_+(\eta_\parallel) = f(\eta_\parallel) f_F(\eta_\parallel), \tag{11}$$

where $f(\eta_\parallel)$ is the initial longitudinal profile (9) fitted to reproduce $dN/d\eta$, and

$$f_F(\eta_\parallel) = \begin{cases} 0 & \eta_\parallel < -\eta_m \\ \frac{\eta_\parallel + \eta_m}{2\eta_m} & -\eta_m \leqslant \eta_\parallel \leqslant \eta_m \\ 1 & \eta_m < \eta_\parallel \end{cases}. \tag{12}$$

The initial energy density of the fireball is constructed as a sum of three terms originating from the forward- or backward-moving participant nucleons and from the binary collisions that are assumed to contribute in a symmetric way:

$$\epsilon(\tau_0) = \epsilon_0\{2[N_+(x,y) f_+(\eta_\parallel) + N_-(x,y) f_-(\eta_\parallel)](1-\alpha) + 2\alpha N_{\rm bin}(x,y) f(\eta_\parallel)\}/N_0. \tag{13}$$

The net result of the difference between forward and backward emission is a tilt of the source in the x-$\eta_\parallel$ plane (Fig. 3). This breaks the symmetry in the longitudinal direction and generates nonzero directed flow in the expansion.

Hydrodynamic equations in (3 + 1)D

$$\partial_\mu T^{\mu\nu} = 0 \tag{14}$$

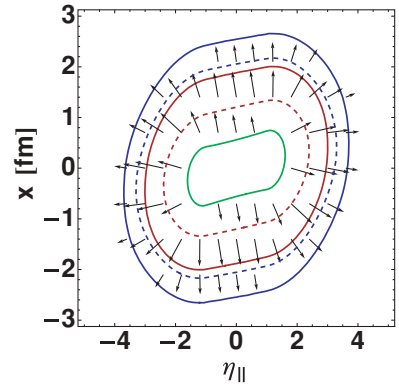

FIG. 3. (Color online) Same as in Fig. 1, but for tilted initial conditions [Eq. (13)].

constitute four independent equations that, together with the equation of state, determine the evolution of the energy density ϵ, of the pressure p, and of three independent components of the fluid velocity. The fluid four velocity can be written in the form

$$u^\mu = (\gamma \cosh Y, u_x, u_y, \gamma \sinh Y), \tag{15}$$

where u_x and u_y are the components of the transverse velocity, $\gamma = (1 + u_x^2 + u_y^2)^{1/2}$ and $Y = \frac{1}{2}\ln(\frac{1+v_z}{1-v_z})$ is the fluid rapidity. The densities are functions of the proper time τ, the space-time rapidity $\eta_\parallel$, and the transverse coordinates x and y. The equations in the expanded form can be found in Ref. [5]. At early times, the velocities on the right-hand side of the equations can be approximated by the initial velocities $u_x = 0$, $u_y = 0$, and $Y = \eta_\parallel$. The two acceleration equations for the velocity components in the reaction plane take the form

$$\begin{aligned} \partial_\tau u_x &= -\frac{1}{\epsilon + p}\partial_x p, \\ \partial_\tau Y &= -\frac{1}{\tau(\epsilon + p)}\partial_{\eta_\parallel} p. \end{aligned} \tag{16}$$

In $(3 + 1)$D hydrodynamic evolution, the lack of Bjorken invariance results in a nonzero longitudinal acceleration. The fluid rapidity Y becomes larger than the space-time rapidity $\eta_\parallel$. Figures 1 and 3 show the vector fields of the initial pressure gradients $(\frac{1}{\tau_0}\partial_{\eta_\parallel} p,\ \partial_x p)$. For the shifted initial conditions, the gradient in the central region of the fireball is in the transverse direction, and mainly transverse flow is generated in the early stage. This is due to the existence of an approximate Bjorken plateau for central rapidities in the initial stage. The situation is different for tilted initial conditions (Fig. 3); the acceleration in the tilted source is anticorrelated in the transverse x and longitudinal $\eta_\parallel$ directions. The matter that is accelerated to positive rapidities is preferably accelerated in the negative x direction. The same figures show the lines of constant pressure for the initial fireball created in Cu-Cu collisions for the same centrality. The deformation for the shifted fireball (Fig. 1), or the tilt for the tilted fireball (Fig. 3), in the smaller system is very similar to that in the larger system. This generates a similar directed flow in the two systems irrespective of their sizes.

III. RESULTS

The hydrodynamic equations are solved numerically for the two sets of initial conditions: the shifted initial distributions given by Eq. (8) and the tilted initial conditions given by Eq. (13). The parameter ϵ_0 is chosen to reproduce particle spectra and multiplicities in central collisions. We use $\epsilon_0 = 107\ \mathrm{GeV/fm^{-3}}$ and $\epsilon_0 = 65\ \mathrm{GeV/fm^{-3}}$ for Au-Au and Cu-Cu collisions, respectively, and a freeze-out temperature of $T_F = 150$ MeV. This gives a satisfactory description of the spectra in collisions up to centralities of 50% [5].

The distribution of charged particles in pseudorapidity is shown in Fig. 4. The results obtained from the two initial conditions are almost indistinguishable on the plot. Both initial conditions lead to similar results for transverse momentum spectra of particles, interferometry radii, and elliptic flow, as well. The comparison with experimental data can be found in Ref. [5], giving satisfactory results. The calculated elliptic flow overshoots the experimental data since we do not take viscosity effects into account [26]. The parameters of the initial profile in space-time rapidity $f(\eta_\parallel)$ are adjusted to reproduce, as closely as possible, the experimental results on pseudorapidity distributions, and transverse momentum spectra at nonzero rapidities [5]. Changing the width η_0 of the plateau in the initial profile $f(\eta_\parallel)$, within a range compatible with the observed pseudorapidity distributions, does not change the results for the directed flow. Only taking the unrealistic value $\eta_0 = 0$ for shifted initial conditions causes the wiggle of positive v_1 to disappear at central pseudorapidities.

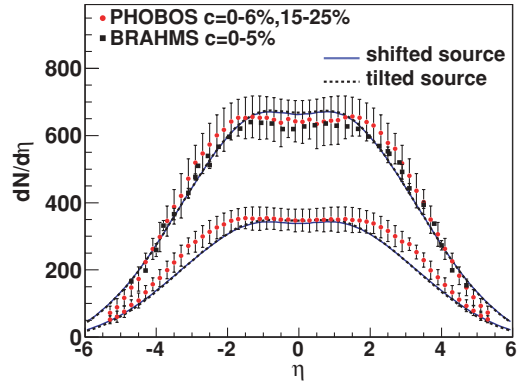

FIG. 4. (Color online) Pseudorapidity distribution of charged particles for centrality classes 0%–6% and 15%–25%, calculated for the shifted and tilted initial conditions (solid and dashed lines, respectively) compared to PHOBOS Collaboration data (dots) [24]. The squares represent the BRAHMS Collaboration data for centrality 0%–5% [25].

By breaking the symmetry in the longitudinal direction, some directed flow can be generated. Figures 5 and 6 show the development of the asymmetric flow in the x direction at different times. The average velocity in the x direction is calculated for a given space-time rapidity and time by

$$\langle v_x \rangle = \frac{\int dxdy v_x \gamma \epsilon}{\int dxdy \gamma \epsilon}. \tag{17}$$

As already mentioned, during the evolution the Bjorken flow $Y = \eta_\parallel$ is modified, but the final flow conserves a strong correlation between Y and $\eta_\parallel$ [5]. Therefore, the directed flow

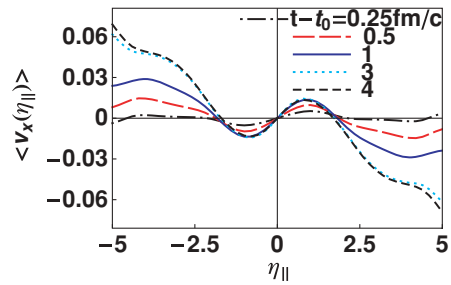

FIG. 5. (Color online) Average flow in the x direction as function of space-time rapidity for different evolution times for the Hirano-Tsuda shifted initial densities [Eq. (8)].

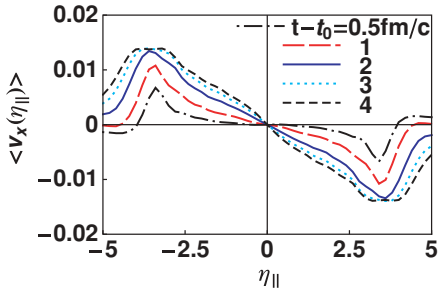

FIG. 6. (Color online) Same as in Fig. 5, but for tilted initial conditions [Eq. (13)].

as functions of space-time rapidity $\eta_\parallel$, as shown in Figs. 5 and 6, reflects qualitatively the final flow of particles.

The first observation is that the directed flow is built up for an extended time during the expansion, in the first 3 fm/c. There is a noticeable difference between the evolution from the shifted and the tilted initial conditions. For the shifted initial conditions (Fig. 5) in the central space-time rapidity region, a positive directed flow develops gradually in the first 1 fm/c. For large rapidities a negative flow is generated in the first 3 fm/c. The directed flow changes sign around $\eta_\parallel = 2$, a behavior very different from the one observed in the experiment. The appearance of the wiggle in the dependence of v_1 on pseudorapidity is a consequence of the form of the initial profile of the pressure (Fig. 1). The pressure gradient has a significant deflection from the transverse direction only in the forward-backward rapidity regions. On the other hand, the tilted initial condition has a smooth tilted pressure gradient that gives a negative-directed flow in a broad range of space-time rapidities (Fig. 6). The antiflow increase for the first 3 fm/c. The negative-directed flow of the fluid, increasing with rapidity, leads to a similar pattern in the directed flow of the final particles.

The hydrodynamic evolution is continued until freeze-out, where particle emission from the freeze-out hypersurface takes place. Statistical emission and resonance decays are performed using the event generator THERMINATOR [27]. Figures 7 and 8 show the results for three representative centralities, for which experimental data for Au-Au collisions have been published. Other experimental data show that, in Cu-Cu interactions, almost the same directed flow is generated as in the larger system if the centrality is chosen to be the same [10]. The directed flow for the shifted initial conditions shown in Fig. 7 has an incorrect dependence on pseudorapidity. For all three centrality classes, the flow is positive in the central rapidity region, and switches to antiflow in the very forward and backward regions. On the same plots are shown the results for Cu-Cu collisions in similar centrality classes. The flow is similar as for the larger system, and hence different than observed experimentally. The similarity between the flow in Au-Au and Cu-Cu systems reflects the similarity in the initial density profiles (Fig. 1).

Figure 8 shows results for the directed flow of charged particles emitted after a hydrodynamic evolution from the tilted initial fireball [Eq. (13)]. The thick solid lines represent the results for Au-Au collisions. The experimental data are

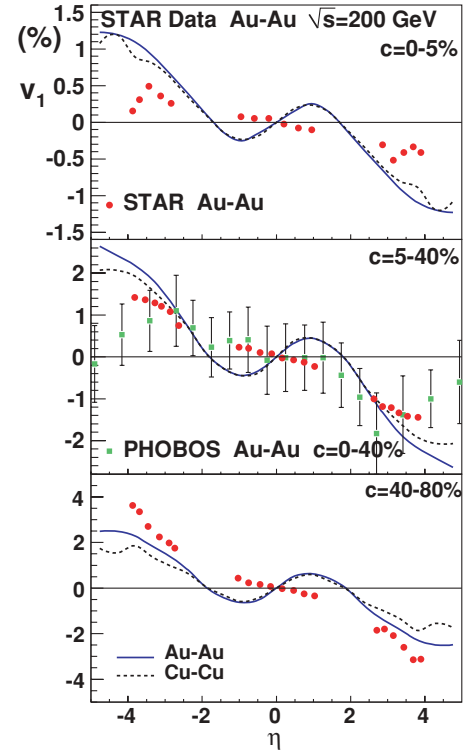

FIG. 7. (Color online) Directed flow at different centralities from hydrodynamic calculations with shifted initial conditions [Eq. (8)] for Au-Au and Cu-Cu collisions (solid and dashed lines, respectively). Experimental data are from the PHOBOS Collaboration [8] for $c = 0\%$–40%, and from the STAR Collaboration [10] for the three other centrality classes.

reproduced in the central rapidity region in a satisfactory way. For the semi-peripheral and peripheral collisions the large antiflow at large pseudorapidities is not reproduced by the model. This kinematic region is at the limit of applicability of the hydrodynamic model, assuming the collective expansion of a thermalized fluid. The directed flow in the fragmentation region can have a different origin, like in the transport models [12]. The panels of Fig. 8 show the results for the Cu-Cu system in the same centrality classes. Again, as expected from the similarity of the tilt of the source in the two systems (Fig. 3), the final directed flows for the two systems almost overlap. To test some of the uncertainty in the choice of the initial conditions for the hydrodynamic evolution, we take as the initial density an ansatz where also the contribution from binary collisions is asymmetric:

$$\epsilon(\tau_0) = 2\epsilon_0 \frac{N_+ f_+(\eta_\parallel) + N_- f_-(\eta_\parallel)}{N_+ + N_-} \times [(1-\alpha)(N_+ + N_-) + 2\alpha N_{\rm bin}]/N_0. \quad (18)$$

The tilt is stronger in this case and the magnitude of the directed flow bigger (thin solid lines in Fig. 8). The shaded bands in the figure represent the uncertainty of the model related to this assumption. This uncertainty is the largest among those that we tested.

In the following, we study the effect of other details of the model on the final directed flow. First, a different initial time

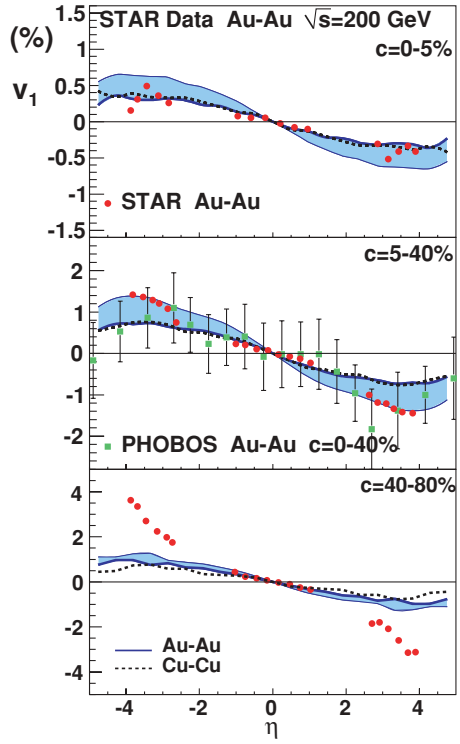

FIG. 8. (Color online) Directed flow in Au-Au (thick solid lines) and Cu-Cu (dashed lines) collisions at different centralities from tilted initial conditions [Eq. (13)], compared to experiment [8,10]. The shaded band between the thin and thick lines represents the increase in the magnitude of the flow if Eq. (18) is used for the initial density, including also asymmetric contributions from binary collisions.

for the hydrodynamic evolution is chosen: $\tau_0 = 1\,\mathrm{fm/c}$. The initial time is given by the rate of the initial thermalization processes that lead to the formation of a dense, almost perfect fluid. The precise mechanisms of thermalization are not known and it is instructive to test the influence of the value of the thermalization time on the build up of the directed flow. Figure 9 shows the result for the centrality class 5%–40%. The directed flow is reduced when compared to the previous calculation using $\tau_0 = 0.25\,\mathrm{fm/c}$. The fluid that starts to expand at $\tau_0 = 1\,\mathrm{fm/c}$ exerts less pressure. In fact, the experimental points for central rapidities lie between the two lines representing the two calculations starting at different thermalization times.

Another effect worth studying is the dependence on the details of the form factor $f_{\pm}(\eta_{\parallel})$, which describes the emission from a single participant nucleon. The range of forward-backward correlations is set by the parameter η_m. We make another calculation using $\eta_m = y_b$. With this choice, the emission from a forward-going participant nucleon decreases when going from rapidity y_b to zero at the rapidity $-y_b$. The initial tilt of the source is smaller than for the choice $\eta_m = y_b - 2$ used before. The effect of this change on the directed flow is small and the results are close to the experimental data at central rapidities (dotted line in Fig. 9).

A third effect that can be tested is the assumption that the initial energy density is proportional to the density of wounded nucleons (binary collisions), as in Eq. (13). Assuming that this

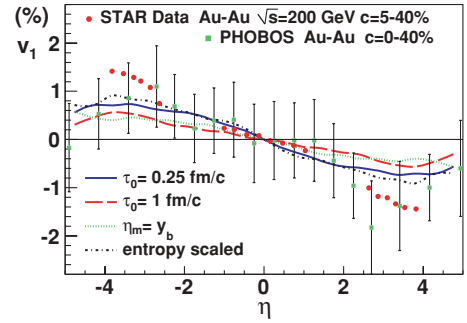

FIG. 9. (Color online) Directed-flow coefficient as function of pseudorapidity for tilted initial conditions ([Eq. (13)] in Au-Au collisions. The solid and dashed lines represent the calculations with initial times $\tau_0 = 0.25$ and 1 fm/c respectively and with an initial profile f_F with $\eta_m = y_b - 2$, the dotted line is for $\tau_0 = 0.25$ fm/c but $\eta_m = y_b$, and the dashed-dotted line represents the result of a calculation where the initial entropy density is proportional to the density of participants from the Glauber model. Data are from Refs. [8,10].

proportionality applies to the entropy density s instead, we have

$$s(\tau_0) = s_0\{[N_+(x,y)f_+(\eta_{\parallel}) + N_-(x,y)f_-(\eta_{\parallel})](1-\alpha) + 2\alpha N_{\mathrm{bin}}(x,y)f(\eta_{\parallel})\}/N_0\,. \quad (19)$$

The directed flow is very similar to the one obtained using the energy density initial profile given by Eq. (13) (dashed-dotted line in Fig. 9). We notice that some of the details of the initial conditions can influence the final directed flow. This situation resembles the conclusion from the elliptic-flow studies, where a crucial ingredient is the initial eccentricity of the fireball.

IV. SUMMARY

We study the formation of the directed flow in the (3 + 1)D hydrodynamic expansion of the fireball created in heavy-ion collisions at the highest energies at RHIC. The directed flow of charged particles has been measured as function of pseudorapidity, finding a substantial negative flow [8–10]. We use two different initial conditions for the evolution. The first one [Eq. (8)] is quite commonly used in hydrodynamic model calculations [4]. It incorporates a shift of the densities in the initial fireball that are due to the local imbalance of the longitudinal momentum. Initial densities of the second type are constructed as a sum of contributions from forward- and backward-going participants [Eq. (13)]. The asymmetry in the emission from individual participants leads to a tilt of the source. Model calculations, incorporating a hydrodynamic expansion stage, particle emission at freeze-out, and resonance decays, indicate that the second type of initial conditions can reproduce the sign and the magnitude of the observed directed flow at central rapidities.

The large negative flow close to the fragmentation regions is of different origin and cannot be described in our calculation. Deviations from the Bjorken flow in the initial conditions [28] could influence the results. In particular, they could lead to a different flow pattern for baryons and for the bulk of the matter, if baryons do not follow the Bjorken flow. The directed

flow is expected to decrease with the collision energy for two reasons. With increasing kinematic range of rapidities the tilt of the source goes down, also the contribution of binary collisions to the Glauber-model density is believed to increase with the energy, with a similar consequence. Finally let us note that our calculation reproduces the experimentally observed similarity of the flow in Au-Au and Cu-Cu collisions at the same centrality.

ACKNOWLEDGMENTS

The authors are very grateful to Jean-Yves Ollitrault for correspondence and discussions that have been of vital importance in finding errors in early studies and in reaching the correct conclusions. This work is supported by Polish Ministry of Science and Higher Education under grants N202 034 32/0918 and N N202 263438.

[1] I. Arsene *et al.* (BRAHMS Collaboration), Nucl. Phys. A **757**, 1 (2005); B. B. Back *et al.* (PHOBOS Collaboration), *ibid.* **757**, 28 (2005); J. Adams *et al.* (STAR Collaboration), *ibid.* **757**, 102 (2005); K. Adcox *et al.* (PHENIX Collaboration), *ibid.* **757**, 184 (2005).

[2] E. Schnedermann, J. Sollfrank, and U. W. Heinz, Phys. Rev. C **48**, 2462 (1993); P. F. Kolb, J. Sollfrank, and U. W. Heinz, *ibid.* **62**, 054909 (2000).

[3] D. Teaney, J. Lauret, and E. V. Shuryak, Phys. Rev. Lett. **86**, 4783 (2001); P. F. Kolb and U. W. Heinz, in *Quark Gluon Plasma 3*, edited by R. Hwa and X. N. Wang (World Scientific, Singapore, 2004), arXiv:nucl-th/0305084; Y. Hama *et al.*, Nucl. Phys. A **774**, 169 (2006); P. Huovinen and P. V. Ruuskanen, Annu. Rev. Nucl. Part. Sci. **56**, 163 (2006); T. Hirano, U. W. Heinz, D. Kharzeev, R. Lacey, and Y. Nara, Phys. Lett. B **636**, 299 (2006); W. Broniowski, M. Chojnacki, W. Florkowski, and A. Kisiel, Phys. Rev. Lett. **101**, 022301 (2008).

[4] T. Hirano and K. Tsuda, Phys. Rev. C **66**, 054905 (2002).

[5] P. Bożek and I. Wyskiel, Phys. Rev. C **79**, 044916 (2009).

[6] J.-Y. Ollitrault, Phys. Rev. D **46**, 229 (1992).

[7] N. Herrmann, J. P. Wessels, and T. Wienold, Annu. Rev. Nucl. Part. Sci. **49**, 581 (1999); A. Wetzler *et al.* (NA49 Collaboration), Nucl. Phys. A **715**, 583 (2003); S. A. Voloshin, *ibid.* **715**, 379 (2003); M. A. Lisa, U. W. Heinz, and U. A. Wiedemann, Phys. Lett. B **489**, 287 (2000).

[8] B. B. Back *et al.* (PHOBOS Collaboration), Phys. Rev. Lett. **97**, 012301 (2006).

[9] J. Adams *et al.* (STAR Collaboration), Phys. Rev. C **73**, 034903 (2006).

[10] B. I. Abelev *et al.* (STAR Collaboration), Phys. Rev. Lett. **101**, 252301 (2008).

[11] S. A. Voloshin *et al.* (STAR Collaboration), J. Phys. G **34**, S883 (2007).

[12] M. Bleicher and H. Stoecker, Phys. Lett. B **526**, 309 (2002); J. Y. Chen *et al.*, Phys. Rev. C **81**, 014904 (2010).

[13] G. Burau *et al.*, Phys. Rev. C **71**, 054905 (2005).

[14] L. P. Csernai and D. Rohrich, Phys. Lett. B **458**, 454 (1999).

[15] R. P. G. Andrade *et al.*, Acta Phys. Pol. B **40**, 993 (2009).

[16] T. Hirano, K. Morita, S. Muroya, and C. Nonaka, Phys. Rev. C **65**, 061902(R) (2002).

[17] L. M. Satarov, I. N. Mishustin, A. V. Merdeev, and H. Stöcker, Phys. Rev. C **75**, 024903 (2007); P. Bożek, *ibid.* **77**, 034911 (2008).

[18] M. Chojnacki and W. Florkowski, Acta Phys. Pol. B **38**, 3249 (2007).

[19] A. Białas and M. Jeżabek, Phys. Lett. B **590**, 233 (2004); K. Fiałkowski and R. Wit, J. Phys. G **31**, 361 (2005); S. J. Brodsky, J. F. Gunion, and J. H. Kuhn, Phys. Rev. Lett. **39**, 1120 (1977); A. Adil and M. Gyulassy, Phys. Rev. C **72**, 034907 (2005); A. Adil, M. Gyulassy, and T. Hirano, Phys. Rev. D **73**, 074006 (2006).

[20] A. Białas and W. Czyż, Acta Phys. Pol. B **36**, 905 (2005).

[21] A. Bzdak, Phys. Rev. C **80**, 024906 (2009).

[22] M. Gaździcki and M. I. Gorenstein, Phys. Lett. B **640**, 155 (2006).

[23] A. Bzdak and K. Wozniak, Phys. Rev. C **81**, 034908 (2010).

[24] B. B. Back *et al.*, Phys. Rev. Lett. **91**, 052303 (2003).

[25] I. G. Bearden *et al.* (BRAHMS Collaboration), Phys. Rev. Lett. **88**, 202301 (2002).

[26] P. Bożek and I. Wyskiel, PoS **EPS-HEP 2009**, 039 (2009).

[27] A. Kisiel, T. Tałuć, W. Broniowski, and W. Florkowski, Comput. Phys. Commun. **174**, 669 (2006).

[28] R. J. M. Snellings, H. Sorge, S. A. Voloshin, F. Q. Wang, and N. Xu, Phys. Rev. Lett. **84**, 2803 (2000); F. Becattini, F. Piccinini, and J. Rizzo, Phys. Rev. C **77**, 024906 (2008).